Why Does Cp_2YH Catalyze the Polymerization of Ethene but Not of Propene?

Nadja Sändig*,† and Wolfram Koch*,‡

Institut für Organische Chemie, Technische Universität Berlin, Strasse des 17. Juni 135, D-10623 Berlin, Germany

Received May 24, 2001

The mechanistic details of the polymerization of ethene and propene brought about by a dicyclopentadienyl yttriumhydride catalyst have been computationally investigated using approximate density functional theory. In accord with experimental information, the overall reaction sequence $Cp_2YH + 2C_2H_4 \rightarrow Cp_2Y{-}C_4H_9$ and $Cp_2YH + 2C_3H_6 \rightarrow Cp_2Y{-}C_6H_{13}$ is computed to be exothermic by ca. 54.1 and 49.4 kcal mol^{-1}, respectively. The reaction mechanism predicted by our calculations is in harmony with the available experimental information but provides additional information into the various elementary steps of this reaction, which could not be obtained by experimental means.

Introduction

The efficient formation of polymers based on ethene and propene is an important process and has led to much research efforts. The search for catalysts that lower the activation barriers of the polymerization reactions is characterized by many important highlights, most notably the Nobel Prize winning introduction of metal organic Lewis acids as catalysts by Ziegler and Natta.[1] Marks et al.[2] were the first to use highly reactive organometallic compounds containing lanthanoids as catalysts for the polymerization of olefins. Specifically, these authors employed lanthanoid complexes with two pentamethylcyclopentadienyl (Cp*) and a hydride ligand, i.e., Cp^*_2MH (Scheme 1), as catalysts that were accessible via a straightforward synthetic route.

This organolanthanoid hydride reacts further with an olefin without using a cocatalyst. The monomer inserts into the bond between the metal and the hydrogen. Subsequently, additional olefin molecules insert between the lanthanoid and the now steadily increasing chain by the same mechanism as summarized in Scheme 2.

This catalyst and the corresponding olefin polymerization for monomers such as ethene, propene, and styrene were investigated for its activity and selectivity by Schumann et al.[2] with some astonishing results. Ethene reacts to polyethene within seconds by using cyclohexane or toluene as solvents under room temperature and standard pressure. In contrast to these results, all attempts to polymerize propene via the same procedure produced only what appeared to be traces of oligomers. Pressurized reactions in cyclohexane solution were no more successful. There is no straightforward explanation for this surprising result; however, it is expected that the reason for this behavior is that a η^3-bonded allyl species will be formed as an intermediate which cannot polymerize further by this mechanism. In any event, the underlying reason *why* the catalyst does not support the continuation of the process in the case of propene is not known. Possible reaction paths for the formation of polypropylene from propene using Cp^*_2-MH catalysts and the formation of a η^3-bonded species as a dead-end for the polymerization in the case of propene are depicted in Scheme 3.

Scheme 1 . A Cp^*_2MH Complex

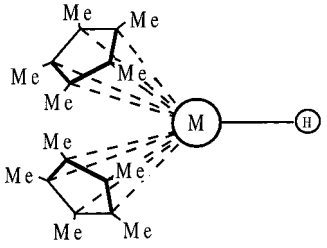

In principle, quantum chemical investigations lend themselves as an ideal complement to experimental works in order to shed more light on such complex mechanistic questions, and many successful examples for the interplay between experiment and theory exist from transition metal, in particular 3d-metal,[3] chemistry. However, quantum chemical calculations for lanthanoid metal compounds are less straightforward. They typically face many problems and pose great demands on the method applied. In the following, we will circumvent these problems by replacing the lanthanoid metal in the Cp^*_2MH catalyst by an yttrium atom, a

* Corresponding author. E-mail: nadja@impact.dyn.unipg.it.
† Present address: Dipartimento di Chimica, Università di Perugia, Via Elce di Sotto 8, I-06123 Perugia, Italy.
‡ Present address: Gesellschaft Deutscher Chemiker e.V., Varrentrappstr. 40−42, D-60486 Frankfurt a.M., Germany.

(1) (a) Ziegler, K. *Adv. Organomet. Chem.* **1968**, *6*, 1, *Nobel Prize Lectures Chemistry* 1963−1970, Elsevier: Amsterdam, 1972. (b) Ziegler, K.; Holzkamp, E.; Breil, H.; Martin, H. *Angew. Chem.* **1955**, *67*, 541. (c) Natta, G.; Pino, P.; Corradini, F.; Mantica, E.; Mazzanti, G.; Moraglio, G. *J. Am. Chem. Soc.* **1955**, *77*, 1708.

(2) (a) Jeske, G.; Lauke, H.; Mauermann, H.; Swepston, P. N.; Schumann, H.; Marks, T. J. *J. Am. Chem. Soc.* **1985**, *107*, 8091. (b) Jeske, G.; Schock, L. E.; Swespston, P. N.; Schumann, H.; Marks T. J. *J. Am. Chem. Soc.* **1985**, *107*, 8103. (c) Jeske, G.; Lauke, H.; Mauermann, H.; Schumann, H.; Marks, T. J. *J. Am. Chem. Soc.* **1985**, *107*, 8111.

(3) Koch, W.; Hertwig R. H. In *The Encyclopedia of Computational Chemistry*; Schleyer, P. v. R., Editor-in-Chief; Wiley: Chichester, 1998.

10.1021/om0104417 CCC: $22.00
Publication on Web 03/26/2002

Scheme 2 . Postulated Mechanism of the Ethene Polymerization

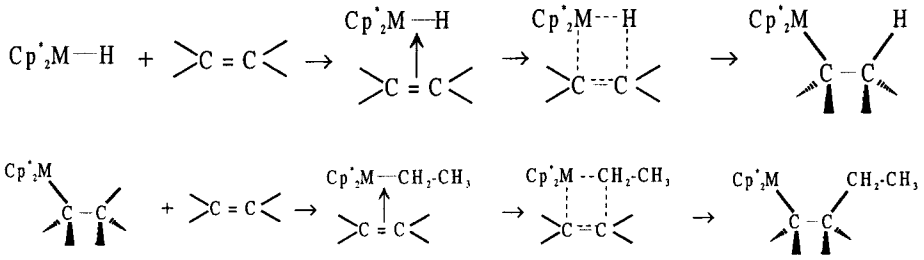

Scheme 3 . Postulated Mechanism of the Propene Reaction

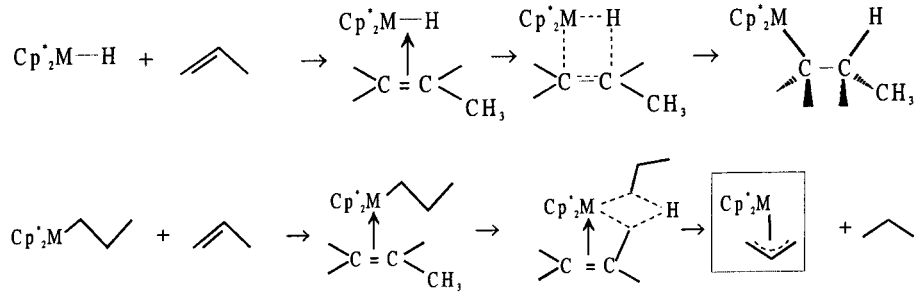

4d-transition metal. Experimentally it is well established that Y behaves very similarly to most lanthanoids, which is mostly due to the lanthanoid contraction. The ionic radii (M^{3+}) of the lanthanoids ranges from 115 (Ce) to 100 pm (Lu); Y's ionic radius amounts to 104 pm.[4] As a second computational simplification we chose to use unsubstituted cyclopentadienyl ligands for the calculations instead of the permethylated Cp* ligand. This can easily be rationalized because the methyl groups of the Cp-ring do not noticeably contribute to the polymerization mechanism. Rather, they are mostly important from an experimental point of view to obtain reasonable solvation properties. Test calculations on the catalysts Cp^*_2Y-H and Cp_2Y-H and the monomer−catalyst compounds $Cp^*_2Y-C_2H_5$ and $Cp_2Y-C_2H_5$ indeed indicate that using Cp instead of Cp* significantly changes neither the charge distribution nor the geometrical features of these species. For example, the NBO partial charge of the yttrium center changes only slightly when going from Cp_2Y-H to Cp^*_2Y-H (from +1.89 to +1.94) and from $Cp_2Y-C_2H_5$ to $Cp^*_2Y-C_2H_5$ (from +2.06 to +2.02), respectively. Hence, we expect that the Cp_2YH species is a suitable model for the description of the initial steps of the polymerization reaction.

The detailed reaction mechanisms of the elementary steps of this reaction are not known so far and call for a comprehensive theoretical investigation. The following study concentrates on the second part of this reaction, i.e., the formation of the dimer−catalyst complex. The first part, namely, the initial insertion of an ethene or propene into the Y−H bond of the catalyst, yielding the monomer−catalyst complex, was already described in detail using a very similar computational approach in a recent investigation.[5] Together with the previous results, we will in this study provide a complete and consistent picture of the ethene polymerization and answer the question why propene does not react to polypropene.

Computational Details

Our computational strategy is based on standard approximate density functional theory.[6] The construction of an appropriate Kohn−Sham Slater determinant and the subsequent geometry optimization of a system of this size are computationally very demanding. That is why we chose a stepwise procedure. All structures were first optimized employing the gradient-corrected exchange−correlation functional by Becke and Perdew[7] combined with the polarized double-ζ DZVP basis set[8] as implemented in the program DGAUSS.[9] In the following this level of calculation will be called BP/BS1. The so generated initial structures were reoptimized by using the popular B3LYP-hybrid functional[10] in connection with a large and flexible relativistic effective core potential (RECP)/valence electron basis set combination by Andrae et al.[11] For these calculations we used Gaussian 98.[12] The RECP represents the 28 core electrons (1s−3d) of yttrium. The remaining 11 valence electrons ($4s^24p^65s^24d^1$) were described by the construction (8s7p7d1f) → (6s5p3d1f)/[311111|22111|4111|1]. The carbon and the hydrogen atoms were characterized by the standard polarized basis set 6-311G**.[13] This combination of density functional and RECP/valence basis set will be designated as B3LYP/BS2 and is the same as used previously in ref 5. For all structures the force constant matrix was computed analytically to establish the character of the stationary points as minima or saddle points. The resulting harmonic

(4) Shannon, R. D. *Acta Crystallogr.* **1976**, *A32*, 751.
(5) Sändig, N.; Dargel, T. K.; Koch, W. *Z. Anorg. Allg. Chem.* **2000**, *626*, 392.
(6) Koch, W.; Holthausen, M. C. *A Chemist's Guide to Density Functional Theory*; Wiley-VCH: Weinheim, 2000.
(7) Perdew, J. P. *Phys. Rev. B* **1992**, *45*, 13244.
(8) Godbout, N.; Salahub, D. R.; Andzelm, J.; Wimmer, E. *Can. J. Chem.* **1992**, *70*, 560.
(9) *DGAUSS* version 4.1; Oxford-Molecular, Inc.: Beaverton, OR, 1998. (a) Dixon, D. A.; Andzelm, J.; Fitzgerald, G.; Wimmer, E.; Jasien, P. In *Density Functional Methods in Chemistry*; Labanowski, J. K., Andzelm, J. W., Eds.; Springer-Verlag: New York, 1991. (b) Andzelm, J.; Wimmer, E. *J. Chem. Phys.* **1992**, *96*, 1280. (c) Chen, H.; Krasowski, M.; Fitzgerald, G. *J. Chem. Phys.* **1993**, *98*, 8710. (d) Komornicki, A.; Fitzgerald, G. *J. Chem. Phys.* **1993**, *98*, 1398.
(10) (a) Becke, A. D. *J. Chem. Phys.* **1993**, *98*, 5648. (b) Becke, A. D. *J. Chem. Phys.* **1993**, *98*, 1372. (c) Stephens, P. J.; Devlin, J. F.; Chabalowski, C. F.; Frisch, M. J. *J. Phys. Chem.* **1994**, *98*, 11623.
(11) Andrae, D.; Haeussermann, U.; Dolg, M.; Stoll, H.; Preuss, H. *Theor. Chim. Acta* **1990**, *77*, 123.

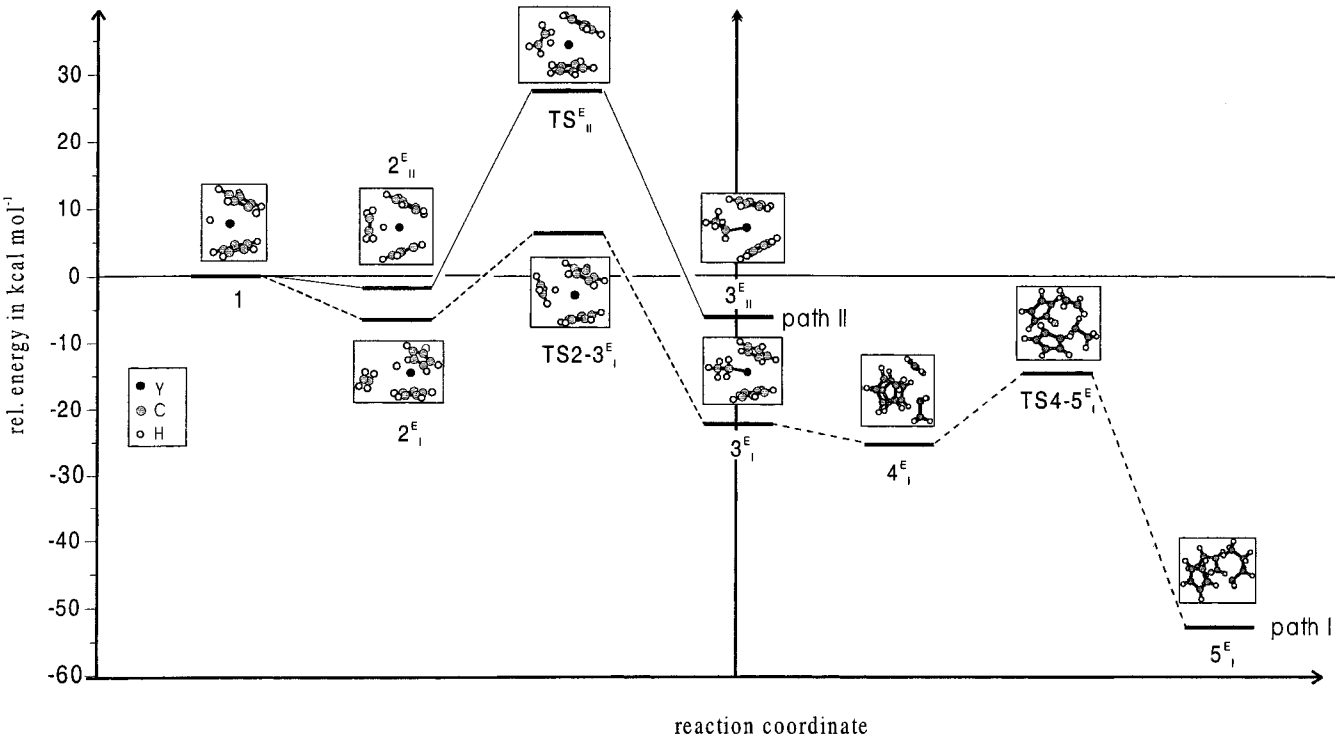

Figure 1. Potential energy surface for the formation of the ethene dimer, $Cp_2YH + 2C_2H_4 \rightarrow Cp_2YC_4H_9$.

frequencies were combined with standard statistical thermodynamics to obtain ΔG^{298K} values which can be directly compared with experimental data.[14] Bond lengths and angles are specified in angstroms (Å) and degrees (deg). While spin-free, kinematical relativistic effects are covered en-gros through the RECP, an additional source of error is introduced by the neglect of spin−orbit interactions in our calculations. However, since we will exclusively deal with ground state singlet species, spin−orbit effects will be of only minor importance. Overall, we expect that our computational strategy furnishes results with error bars on the order of some ±5 kcal mol^{-1}.[6] The natural bond orbital (NBO) method[15] of Weinhold and coworkers was used to extract partial atomic charges and details of the binding situations[16] from the B3LYP/BS2 results.

Results and Discussion

Cp_2YH + 2 Ethene. In this section the results of the different steps of the reaction of ethene with the model catalyst, Cp_2YH, will be discussed. The analogous reaction sequence of propene will be the subject of the following section.

Table 1. Relative Energies in kcal mol^{-1} for the Reaction $Cp_2YH + 2C_2H_4 \rightarrow Cp_2YC_4H_9$

species	path I	path II
1	0	0
$\mathbf{2^E}$	−6.0.5	−1.8
TS2−3^E	6.7	27.8
$\mathbf{3^E}$	−22.2	−6.1
$\mathbf{4^E}$	−25.6	
TS2−5^E	−14.9	
$\mathbf{5^E}$	−54.1	

Figure 1 shows the potential energy surface of all relevant minima and transition structures in their ground state. The calculated energies are given in Table 1. The relative energies are shown with respect to the entrance channel of the reaction $Cp_2YH + 2C_2H_4$, which is defined as 0 kcal mol^{-1}. All structures have closed shell, singlet ground states, and the geometries of the intermediates and saddle points of the second reaction sequence are pictured in Figure 2.

While Figure 1 and Table 1 also include the first reaction sequence, the detailed discussion will concentrate only on the second part of the reaction. The first step, i.e., the formation of the monomer−catalyst complex, has been discussed previously[5] and will be merely briefly recapitulated.

The entrance channel of the first step of the polymerization consists of the reactants ethene and the catalyst, dicyclopentadienylyttriumhydride **1**. These molecules approach each other to form a weakly π-coordinated olefin−metal complex $\mathbf{2^E}$.[17] From this encounter complex, where the reactants are mostly intact, the reaction proceeds to form the catalyst−monomer com-

(12) Frisch, M. J.; Trucks, G. W.; Schlegel, H. B.; Scuseria, G. E.; Robb, M. A.; Cheeseman, J. R.; Zakrzewski, V. G.; Montgomery, J. A., Jr.; Stratmann, R. E.; Burant, J. C.; Dapprich, S.; Millam, J. M.; Daniels, A. D.; Kudin, K. N.; Strain, M. C.; Farkas, O.; Tomasi, J.; Barone, V.; Cossi, M.; Cammi, R.; Mennucci, B.; Pomelli, C.; Adamo, C.; Clifford, S.; Ochterski, J.; Petersson, G. A.; Ayala, P. Y.; Cui, Q.; Morokuma, K.; Malick, D. K.; Rabuck, A. D.; Raghavachari, K.; Foresman, J. B.; Cioslowski, J.; Ortiz, J. V.; Stefanov, B. B.; Liu, G.; Liashenko, A.; Piskorz, P.; Komaromi, I.; Gomperts, R.; Martin, R. L.; Fox, D. J.; Keith, T.; Al-Laham, M. A.; Peng, C. Y.; Nanayakkara, A.; Gonzalez, C.; Challacombe, M.; Gill, P. M. W.; Johnson, B. G.; Chen, W.; Wong, M. W.; Andres, J. L.; Head-Gordon, M.; Replogle, E. S.; Pople, J. A. *Gaussian 98*; Gaussian, Inc.: Pittsburgh, PA, 1998.

(13) Frisch, M. J.; Pople, J. A.; Binkley, J. S. *J. Chem. Phys.* **1984**, *80*, 3265.

(14) (a) Sändig, N.; Koch, W. *Organometallics* **1997**, *16*, 5244. (b) Sändig, N.; Koch, W. *Organometallics* **1998**, *17*, 2344.

(15) (a) Reed, A. E.; Curtiss, L. A.; Weinhold, F. *Chem. Rev.* **1988**, *88*, 899. (b) Glendening, E. D.; Reed, A. E.; Carpenter, J. E.; Weinhold, F. NBO version 3.1 as implemented in Gaussian 98.

(16) Strictly speaking the wave functions used in the analysis correspond to the Kohn−Sham Slater determinants describing the noninteracting reference systems and not the real, interacting species. However, for all practical purposes these wave functions can be analyzed like regular wave functions in conventional ab initio calculations.

(17) The index E on the numbering of the stationary points stands for ethene.

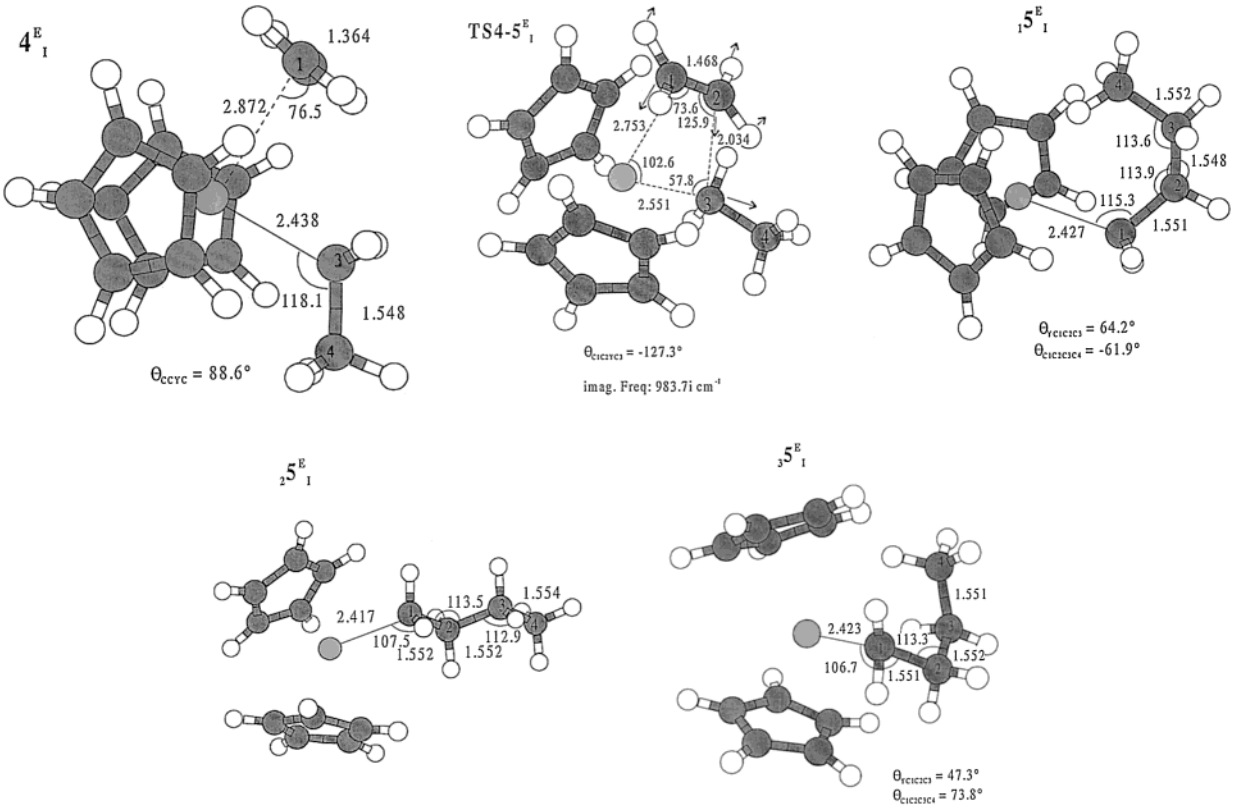

Figure 2. Geometries of all relevant minima and transition structure of the ethene polymerization.

plex $\mathbf{3^E}$. This complex is the starting point of the polymerization. The formation of $Cp_2YC_2H_5$ is connected to an energy barrier which corresponds to the transition structure **TS2**−$\mathbf{3^E}$. For ethene, more than one path leading to the catalyst−monomer complexes had been identified. The overall reaction is exothermic by 22.2 kcal mol^{-1} if we follow path I, the other path being energetically less favorable. The reaction proceeds mainly below the energy of the entrance channel except for the transition state, which lies 6.7 kcal mol^{-1} above the entrance channel or 13.2 kcal mol^{-1} above $\mathbf{2^E}$. Hence, the first reaction sequence has no significant kinetic barrier, in full harmony with the experimental results. The following step of the reaction represents the start of the actual polymerization process. A second ethene molecule reacts with the monomer−catalyst complex and forms a butyl group. This reaction should proceed similar to the first reaction sequence. This means that after the formation of an electrostatically bound encounter complex between the approaching ethene and the monomer−catalyst complex a dimer−(in this case butyl−) catalyst species is expected. The activation barrier connected with this step is significant for the kinetics of this reaction. Unlike in the first part of the reaction, the second ethene molecule will not insert into a hydrogen−yttrium bond, but into a carbon−yttrium bond. As described above, two different products, $Cp_2YC_2H_5$, of the ethene insertion into a Y−H bond were located. Minimum $\mathbf{3^E_I}$ lies 22.2 kcal mol^{-1} below the entrance channel, in contrast to minimum $\mathbf{3^E_{II}}$, which is merely 6.1 kcal mol^{-1} more stable than the energetical sum of the reactants. Likewise the transition structure calculated for path I is only 6.7 kcal mol^{-1} above the entrance channel, while the saddle point of path II is 27.8 kcal mol^{-1} above the reactants. This shows clearly that reaction path I and minimum $\mathbf{3^E_I}$ are preferred over reaction path II. Hence, we have limited the calculations for the second reaction sequence to following path I only.

The interaction between $\mathbf{3^E_I}$ and the second ethene leads to an electrostatically bound encounter complex $\mathbf{4^E_I}$. Small covalent contributions are reflected in the lengthening of the CC bond in ethene of 0.016 Å[18] and of the yttrium−ethyl bond of 0.078 Å. The ethene moiety is located almost perpendicular ($\theta_{CCYC} = 88.6°$) to the Y−C bond of the catalyst. The distance between the yttrium atom and the incoming ethene amounts to 2.872 Å. This encounter complex lies 25.6 kcal mol^{-1} below the entrance channel, $Cp_2YH + 2C_2H_4$, and is 3.4 kcal mol^{-1} more stable than the reactants of the second part of the reaction $Cp_2YC_2H_5 + C_2H_4$. Stepping further along the reaction path, the product $Cp_2YC_4H_9$ will be generated by the insertion of the ethene molecule into the Y−C bond of the monomer species. This dicyclopentadienyl yttrium butyl species can be formed in three different conformations, $\mathbf{{}_15^E_I}$, $\mathbf{{}_25^E_I}$, and $\mathbf{{}_35^E_I}$.[19] The energetically most favored variant is being realized in $\mathbf{{}_15^E_I}$. It is located 54.1 kcal mol^{-1} below the entrance channel of the whole reaction. However, the other two minima $\mathbf{{}_25^E_I}$ and $\mathbf{{}_35^E_I}$ are merely 0.9 and 1.4 kcal mol^{-1} less stable than $\mathbf{{}_15^E_I}$. Considering the expected errors

(18) The C−C distance in free ethene amounts to 1.348 Å.

(19) A description of the nomenclature on the example of the minimum $\mathbf{{}_15^E_I}$:

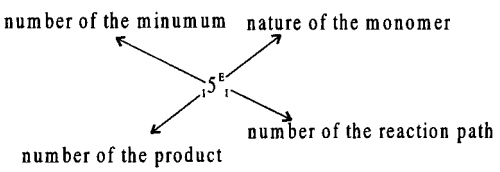

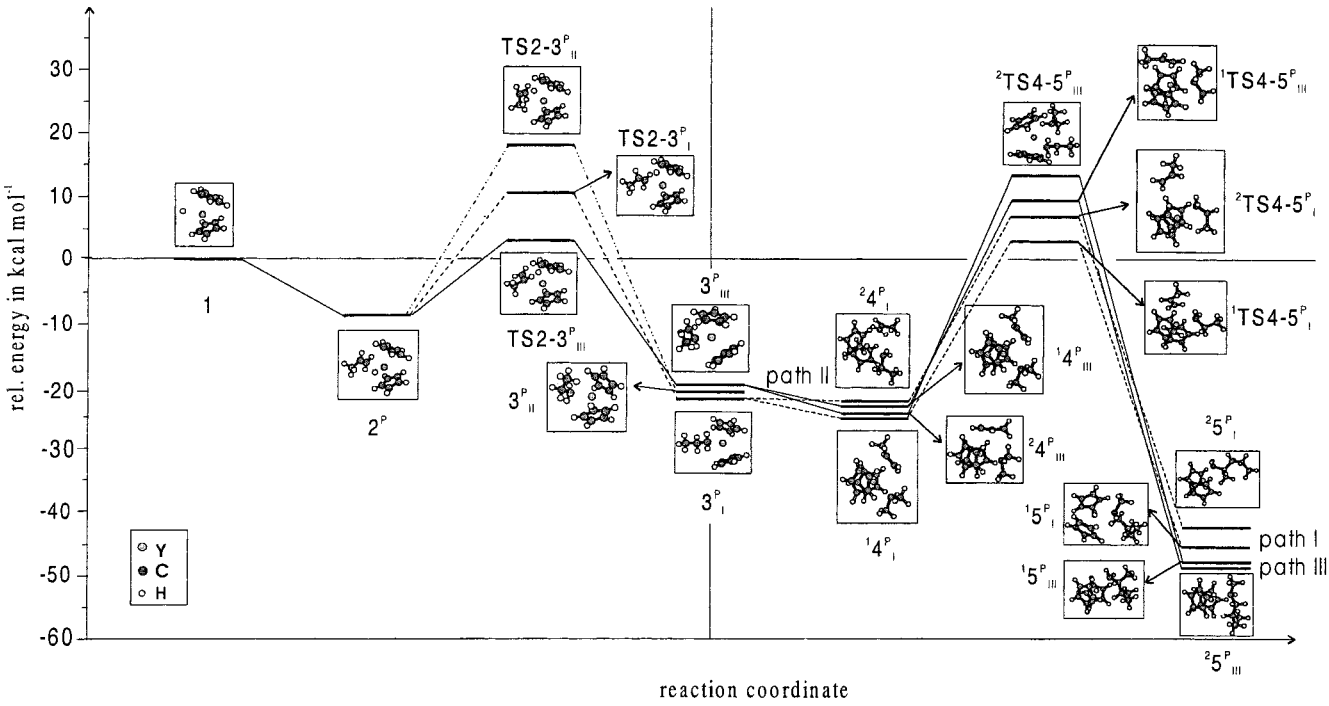

Figure 3. Potential energy surface for the formation of the propene dimer, $Cp_2YH + 2C_3H_6 \rightarrow Cp_2YC_6H_{13}$.

of our computational scheme of ca. 5 kcal mol^{-1}, these energetical differences are too small to unequivocally define the energetically lowest lying conformation. Hence, all three minima must be classified as more or less isoenergetic. The structures of these three stationary points differ in particular in the torsion angles $\theta_{YC1C2C3}$ and $\theta_{C1C2C3C4}$. The butyl group of $_15^E_I$ is located such that the terminal carbon atom is opposite to the metal center. The yttrium−carbon distance amounts to 2.427 Å and the C−C bond lengths are ca. 1.55 Å, indicative for formal single bonds. The YC1C2 angle was optimized to 115.3°, and the C1C2C3 and C2C3C4 angles of the butyl group were optimized to 113.9° and 113.6°, respectively. The $\theta_{YC1C2C3}$ torsion angle of this minimum was calculated to 64.2° and $\theta_{C1C2C3C4}$ to −61.9°. In comparison to minimum $_15^E_I$ the carbon atoms of the butyl group in $_25^E_I$ are located in the C_s mirror plane of the catalyst. Both torsion angles amount to 180°. The C_4H_9 group is 2.417 Å away from the yttrium atom, and the distances between the carbon atoms are all on the order of some 1.55 Å. The YC1C2 angle has been computed as 107.5°, and the angle between the C atoms as 113.5° and 112.9°, respectively. Thus, there is a classical head−tail picture of a catalyst with an increasing polymer chain. The last minimum $_35^E_I$ is very similar to $_15^E_I$, the main difference being the torsion angles: The YC1C2C3 angle, 47.3°, is much smaller than the corresponding angle in $_15^E_I$, while the C1C2C3C4 dihedral angle was calculated as 73.8° ($_15^E_I$: $\theta_{YC1C2C3} = -61.9°$). The terminal methyl group points away and not toward the yttrium atom. All three minima are related to each other through rotations around the C−C axes of the butyl group. The transition structures of these rotations were not optimized. They are expected to be very small (certainly not more than a few kcal mol^{-1}) and hence will have no significant impact on the reaction mechanism. Decisive for the second step of the reaction is the transition structure that connects 4^E and $_15^E_I$, i.e., **TS4**−5^E_I. It lies 14.9 kcal mol^{-1} below the entrance channel and 10.7 kcal mol^{-1} above 4^E_I. Thus no significant kinetic barriers exist in this reaction sequence, in good agreement with the experimental results of Schumann and co-workers.[2] **TS4**−5^E_I was clearly characterized as a saddle point by a single imaginary frequency of 983.7i cm^{-1} with transition vectors pointing into the expected directions. Also intrinsic reaction coordinate (IRC) calculations confirm the direct connection between **TS4**−5^E_I and minima 4^E and $_15^E_I$. In **TS4**−5^E_I the mechanism can be described as a kind of metathesis reaction. Two bonds (YC_{ethyl} and the double bond of the ethene) are broken while at the same time two new bonds (YC_{ethene} and $C_{ethyl}C_{ethene}$) are being formed via a four-membered ring system, as indicated by the lengthening of the YC_{ethyl} ($\Delta r_{YC} = 0.113$ Å) and C=C ($\Delta r_{CC} = 0.136$ Å) bonds and the concomitant shortening of the YC_{ethene} ($\Delta r = -0.119$ Å) and C_{ethyl}-C_{ethene} ($\Delta r_{CC} = -1.547$ Å) bonds compared to 4^E.

Table 2. Relative Energies in kcal mol^{-1} for the Reaction $Cp_2YH + C_3H_6 \rightarrow Cp_2YC_6H_{13}$

species	path I	path II	path III	
1	0	0	0	
2^P	−9.0	−9.0	−9.0	
TS2−3^P	10.7	18.4	3.8	
3^P	−21.6	−20.9	−19.5	
4^P	−22.0	−25.3	−22.9	−24.4
TS2−5^P	−14.9	7.1	9.5	12.9
5^P	−54.1	−46.3	−49.4	−48.7

Cp_2YH + 2 Propene. A summary of the three different reaction paths leading to the dimer−catalyst complex is shown schematically in the potential energy surface of the reaction $Cp_2YH + 2C_3H_6$ (Figure 3). The geometries of all relevant minima and saddle points of the second reaction sequence are given in Figure 4. Table 2 contains the computed relative energies of the electronic ground states of the relevant structures. The entrance channel consists of the reactants Cp_2YH and $2C_3H_6$ and defines 0 kcal mol^{-1}.

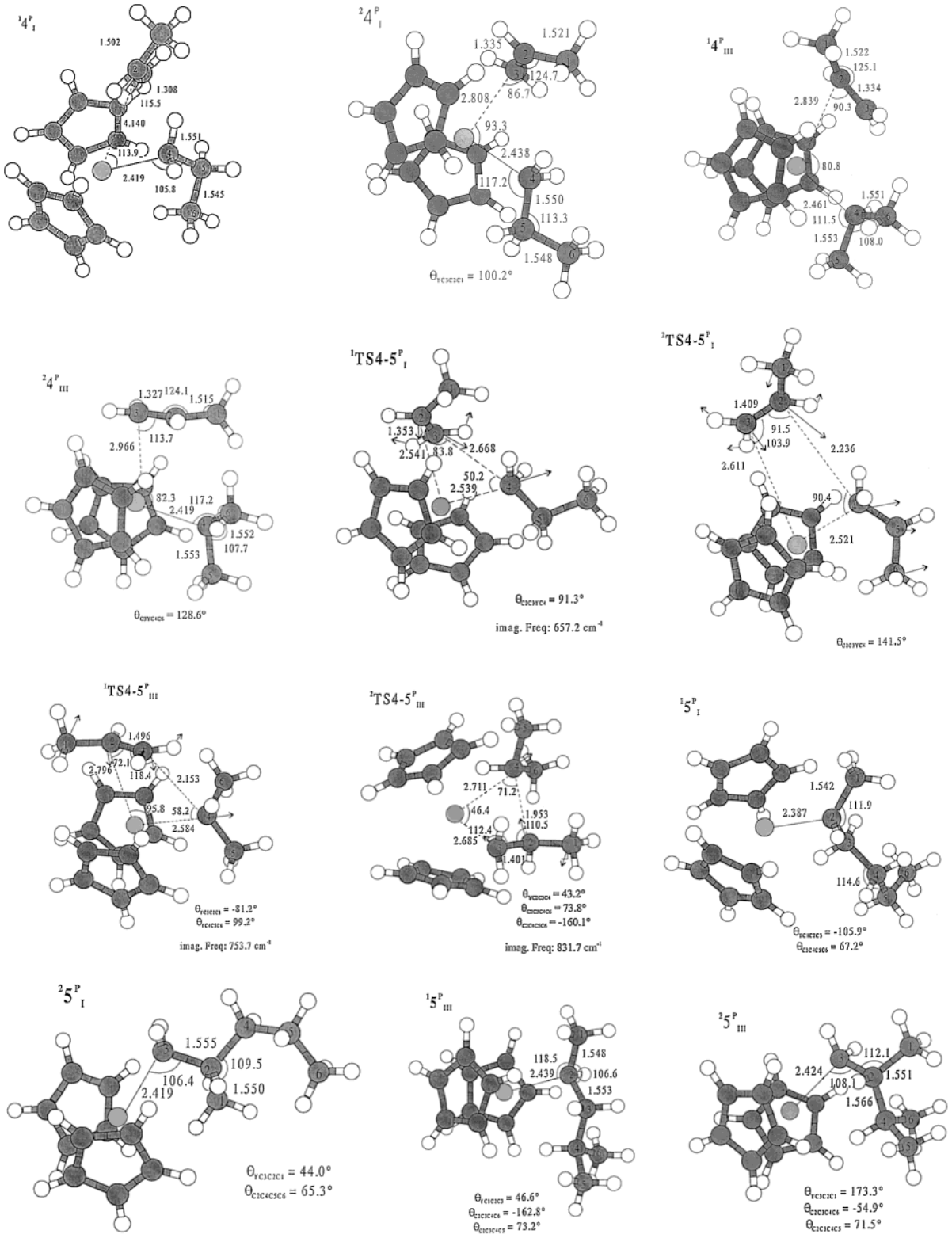

Figure 4. Geometries of all relevant minima and transition structure of the propene reaction.

Figure 3 and Table 2 include again also the first reaction sequence, which was already discussed in detail in ref 5. In the following only a short summary of these results is given.

The reaction mechanism of the first sequence, i.e., the formation of the monomer−catalyst complex, is very similar to the ethene reaction. In the first step a π-coordinated encounter complex between the incoming propene molecule and the catalyst is formed. This reacts further to the product $Cp_2YC_3H_7$. Three different but energetically very similar reaction paths were located for this transformation. Of the corresponding three saddle points, one, namely, **TS2**−$\mathbf{3^P_{III}}$, is only 3.8 kcal mol^{-1} above the entrance channel. The other two transition structures, **TS2**−$\mathbf{3^P_I}$ and **TS2**−$\mathbf{3^P_{II}}$, are much higher in energy, and hence it is assumed that the first part of the reaction will proceed along path III. Following this path a Y-shaped form of the yttrium-bonded

propyl group, an isopropyl group, will form. In ref 5 we speculated that this will create steric problems for the insertion of the next propene. Hence, the polymerization in case of propene would be hindered. To confirm this prediction, we computed the reaction pathways leading to the dimer. As outlined above, we characterized path III as the most favorable one. The saddle point connected with path I is 6.9 kcal mol^{-1} higher in energy, and this path was also included in the present study. Only path II, whose activation barrier is another 7.7 kcal mol^{-1} less favorable, was not considered any further.

If a second propene molecule approaches species **3**, two possibilities of the arrangement of the methyl group are conceivable: the CH_3 group of the propene can point either to the metal center or to the bonded propyl group. We will indicate the first case in the symbol of the minima and transition structures with an index '1' and the second case with an index '2'.[20] It will turn out that there are four different structures for every stationary point. In the following we will discuss these structures according to the reaction paths I and III.

Path I. As outlined above, this path is characterized by an energy barrier of 10.7 kcal mol^{-1} in the first step (with respect to the entrance channel, 19.7 kcal mol^{-1} with respect to $\mathbf{2^P}$) and will for that reason probably not qualify as a probable path for the polymerization reaction. We have nevertheless included this path in our investigation of the subsequent step to elucidate the energetics of the relevant intermediates and saddle points. Two different encounter complexes will be formed by the interaction of a second propene molecule with the initial complex. Both minima, −22.0 and −25.3 kcal mol^{-1} for $\mathbf{^1 4^P_I}$ and $\mathbf{^2 4^P_I}$, respectively, lie below the entrance channel of the whole reaction and are thus 0. and 3.7 kcal mol^{-1}, respectively, more stable than the reactants of the second sequence, $Cp_2YC_3H_7 + C_3H_6$. In the encounter complex $\mathbf{^1 4^P_I}$ both sp^2-hybridized carbon atoms of the propene moiety can interact with the yttrium. The central carbon atom points toward the metal center. The distance between the yttrium atom and this carbon atom amounts to 4.140 Å. This large distance is typical for a purely electrostatical interaction. While the bonds within the propene molecule are almost unchanged, the Y−C4 distance lengthens by 0.011 Å. The propyl group is still in the C_s plane of the catalyst. The second propene inserts more or less (α_{C3C2Y} = 115.5°) from "above" into the yttrium−propyl bond. The second electrostatic encounter complex, $\mathbf{^2 4^P_I}$, has a very similar structure. Also here the double bond of the propene is almost perpendicular to the $Y-C_3H_7$ bond of the monomer−catalyst complex. The carbon atom of the propene methyl group has a distance of only 2.808 Å to the metal atom. This Y−C distance is much smaller than the r_{YC} = 4.140 Å found for $\mathbf{^1 4^P_I}$. The propene double bond is lengthened by 0.027 Å, the $Y(C_3H_7)$ bond by 0.03 Å, and the single bond in propene by 0.019 Å. Proceeding along the reaction coordinate, the minima $\mathbf{^1 5^P_I}$ and $\mathbf{^2 5^P_I}$ will be formed next. They are the final products for path I of the second sequence. Both minima, −47.8 and −46.3 kcal mol^{-1} with respect to the entrance channel $Cp_2YC + 2C_3H_6$, are very exothermic products. In the first of these products, $\mathbf{^1 5^P_I}$, dicyclopentadienyl-yttrium-(1-methylpentyl), the two carbon atoms of the propene double bond have inserted into the yttrium−propyl bond. The methyl group of the propene is now located in the α-position of the pentyl chain with respect to the yttrium atom. The distance between the metal and the closest carbon atom amounts to 2.387 Å. The carbon chain moved outside the C_s plane of the catalyst. The YC1C2C3 torsion angle is 105.9° and that to the following propyl group 67.2°. Also in $\mathbf{^2 5^P_I}$, dicyclopentadienylyttrium-(2-methylpentyl), a pentyl chain where the methyl group is situated at position 2 is formed. The distance between the metal center and the first carbon atom, 2.419 Å, is a bit longer than in $\mathbf{^1 5^P_I}$. The torsion angle of the yttrium−C1C2C3 unit has been computed as 44°, and the corresponding angle with respect to the rest of the chain as 65.3°.

Both products are in the exothermic area. The transition structures connected with the conversion from $\mathbf{4^P_I}$ to $\mathbf{5^P_I}$, i.e., $\mathbf{^1TS4-5^P_I}$ and $\mathbf{^2TS4-5^P_I}$, lie 4.4 and 7.1 kcal mol^{-1} above the entrance channel $Cp_2YH + 2C_3H_6$, respectively, or 26.4 and 32.4 kcal mol^{-1} above $\mathbf{^1 4^P_I}$ and $\mathbf{^2 4^P_I}$, respectively. Hence, we conclude that the reason no polypropene will be formed along path I under standard conditions is indeed mainly $\mathbf{TS2-3^P_I}$ of the first step, which lies 10.7 kcal mol^{-1} above the reactants (or 19.7 kcal mol^{-1} above $\mathbf{2^P}$), while the second step described in this section is energetically less demanding.

Path III. As outlined above, path III was identified as the most favorable reaction path in the first reaction sequence, leading to $\mathbf{3^P_{III}}$ and therefore the most likely candidate for a successful polymerization mechanism. In this species the propyl group is bonded to the metal through the central carbon atom. The prediction stated in ref 5 was that the subsequent reaction of a second propene molecule will be hindered due to steric reasons, and thus the polymerization reaction will be prevented. Also along this reaction path two possibilities for the arrangement of the second propene exist. As in path I, the methyl group is located either at the first or at the second position with respect to the metal center. We localized two different corresponding complexes, $\mathbf{^1 4^P_{III}}$ and $\mathbf{^2 4^P_{III}}$. With respect to the entrance channel of the whole reaction the two complexes are 22.9[1] and 24.4 kcal mol^{-1} more stable than the separated reactants, $Cp_2YH + 2C_3H_6$, and also more stable than the reactants of the second sequence ($Cp_2YC_3H_7 + C_3H_6$) by −3.4 and −4.9 kcal mol^{-1}, respectively. In $\mathbf{^1 4^P_{III}}$, the C2−C3 bond of the approaching propene is lengthened by 0.026 Å and the C1−C2 bond by 0.02 Å. The Y−C4 bond of the catalyst−monomer complex is also elongated by 0.074 Å. The propene double bond is perpendicular to the Y−C bond. The shortest distance between the carbon atoms of the propene and the metal is to the central carbon atom and amounts to 2.839 Å. In the second complex $\mathbf{^2 4^P_{III}}$ the propene approaches parallel to the Y−C4 bond so that the double bond of the propene lies nearly in the C_s plane of the catalyst. In this structure the

(20) A description of the nomenclature on the example of minimum $\mathbf{^2 4^P_I}$:

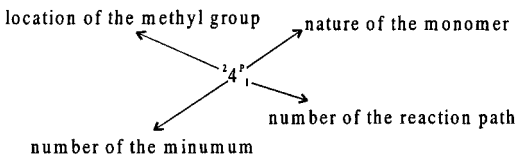

terminal sp^2-hybridized carbon atom (C3) is closest to the yttrium (r_{YC} = 2.966 Å). This is a good position for the methyl group to migrate to the β-position of the chain. Due to the longer distance between the yttrium and the carbon atoms in comparison to **^{1}4$^P_{III}$**, the covalent contribution of the interaction is smaller, as evidenced by the smaller changes in the bond lengths. The C2═C3 double bond increases by 0.016 Å, the C1−C2 single by 0.013 Å, and the Y−C4 bond by 0.032 Å. The following minima **^{1}5$^P_{III}$** and **^{2}5$^P_{III}$** are the final products of the second reaction sequence along path III. They lie 49.4 and 48.7 kcal mol^{-1}, respectively, below the entrance channel of the reaction $Cp_2YH + 2C_3H_6$. Both products are more stable by 1.6 and 2.4 kcal mol^{-1} than the corresponding species on path I. This is not a significant energetical difference, and no prediction about the preferred path can be given at this point. In **^{1}5$^P_{III}$**, dicyclopentadienylyttrium-(1,3-dimethylbutyl), the second propene inserts between the isopropyl group and yttrium. The methyl group of the first propene is bonded to the α-carbon atom of the butyl group which is linked via a σ-bond to the metal center (r_{YC} = 2.439 Å). The propene dimer does not lie in the C_s plane of the catalyst ($\theta_{YC1C2C3}$ = 46.6°). **^{2}5$^P_{III}$** is very similar to **^{1}5$^P_{III}$**. Here the methyl groups are located in the β- and γ-positions. The originally terminal carbon atom C3 of the propene is now bonded to yttrium (r_{YC} = 2.424 Å). Also this species has no symmetry (point group C_1).

If we only consider the energetics of these two minima, no indication of why the polymerization is not observed for propene can be found. Rather, the growing carbon chains arrange such that the steric problems are being avoided. Hence, also in this reaction sequence we need to investigate the transition structures connecting species **4$^P_{III}$** and **5$^P_{III}$**. The two saddle points **^{1}TS4−5$^P_{III}$** and **^{2}TS4−5$^P_{III}$** of the reaction path III are characterized by imaginary frequencies of 753.7i and 831.7i cm^{-1}, respectively, and the transition vectors (indicated in Figure 4) point into the expected directions. **^{1}TS4−5$^P_{III}$** and **^{2}TS4−5$^P_{III}$** lie above the entrance channel of the whole reaction $Cp_2YH + 2C_3H_6$ by 9.5 and 12.9 kcal mol^{-1}, respectively (the effective energy barriers with respect to their direct precursors amount to 32.4 and 37.3 kcal mol^{-1}, respectively), and hence represent significant energetical bottlenecks for the reaction. The modes of the first transition structure, **^{1}TS4−5$^P_{III}$**, show the movement of the incoming propene toward the yttrium−isopropyl bond. In **^{1}TS4−5$^P_{III}$** a four-membered ring structure, typical for a metathesis mechanism, can be identified. Two bonds (C2═C3 of propene and Y−C4 of the catalyst−monomer unit) are broken and two bonds are being formed (Y−C2 and C3−C4), very akin to the corresponding saddle point **^{1}TS4−5^P_I** of path I. In **^{2}TS4−5$^P_{III}$** a very similar situation is being realized. The double bond of the propene and the Y−C4 bond will be broken (Δr_{CC} = 0.074 Å and Δr_{YC} = 0.245 Å) and two new bonds, in this case Y−C3 and C2−C4, will be formed (Δr_{CC} = 0.281 Å and Δr_{YC} = 0.813 Å).

As the general motif of all insertion transition states, a concerted metathesis step can be identified. We therefore assume that also the subsequent polymerization steps will follow the same mechanism with the activation barriers showing similar trends as computed for the first two steps. In all cases the saddle points were computed to lie above the entrance channel. Only one of them, **TS2−3$^P_{III}$**, at +3.8 kcal mol^{-1}, is located in an energetical regime where the reaction could spontaneously happen under standard conditions. However, for the second step, the insertion of the double bond of propene into the yttrium−carbon bond of the catalyst−monomer complex, the transition structures for both possible arrangements of propene lie, at 9.5 and 12.9 kcal mol^{-1}, significantly above the entrance channel of the whole reaction. Hence, due to the activation barriers, the polymerization of propene to polypropene cannot go further than to only the monomer−catalyst complex. This is in very good agreement with the experimental information and provides a quantum chemical answer to the question why the polymerization of propene to polypropene is not being observed in the experiments.

As shown in Scheme 3, the formation of an allyl complex has also been discussed as a possible dead-end for the propene reaction. However, calculations at the BP/BS1 level showed that the resulting exit asymptote, $Cp_2YC_3H_5 + C_3H_8$, lies 24.2 kcal mol^{-1} above the entrance channel. The significant endothermicity of this product channel is an indication that the reaction of $Cp^*_2M-C_3H_7$ with C_3H_6 will not take place, since both alternative reaction paths characterized above are energetically more favorable. The experimentally observed formation of the allyl complex probably follows an alternative path.

Conclusions and Outlook

Density functional calculations employing the B3LYP hybrid functional combined with an adequate one-particle description were carried out in order to identify the mechanisms of the second part of the Cp_2YH-mediated ethene and propene polymerization, i.e., the formation of the catalyst−dimer complex. The reaction sequences consist of several steps, commencing with the formation of a weakly bound encounter complex between the monomer−catalyst and the olefin, followed by the insertion of the ethene or propene into a Y−C bond and finally the formation of a $Cp_2Y-C_4H_9$ or $Cp_2Y-C_6H_{13}$ species. For both olefins, more than one path leading to the catalyst−dimer complexes has been identified. The overall reaction is exothermic by 54.1 kcal mol^{-1} for ethene if path I is followed and 49.4 kcal mol^{-1} for the propene complex if the reaction proceeds along path III, all other paths being energetically less favorable. In both cases, the reaction proceeds mainly below the energy of the entrance channel except for the transition state of the propene polymerization, which lies, at 9.5 kcal mol^{-1}, fairly significantly above the entrance channel. Hence, the ethene reaction has no significant kinetic barrier and should occur spontaneously, in full harmony with the experimental results. In the case of the propene reaction, the originally predicted steric hindrance did not occur. Rather the system is flexible enough to circumvent the unfavorable steric crowding. The reason the propene stops at the monomer−catalyst complex is the height of the activation barrier.

If we assume that the general reaction motif for the first two steps in the olefin polymerization will also apply for the following steps, we can predict that the polymerization of ethene will be characterized by exothermic steps involving a metathesis mechanism with

only small activation barriers. In contrast to this, the transition structure for the polypropene production will be significant above the entrance channel so that the polymerization will not occur under standard conditions.

Acknowledgment. This work was supported by the Deutsche Forschungsgemeinschaft and the Fonds der Chemischen Industrie. A significant amount of computer time and excellent service (Dr. T. Steinke) was provided by the Konrad-Zuse Zentrum für Informationstechnik Berlin. N.S. gratefully acknowledges helpful discussions with Profs. G. Frenking, H. Schumann, and W. Thiel and their co-workers. We thank the anonymous referees for valuable comments.

OM0104417